



Low-dimensionality carbon-based biosensors: the new era of emerging technologies in bioanalytical chemistry

Karla P. R. Castro¹ · Rafael N. P. Colombo¹ · Rodrigo M. Iost¹ · Beatriz G. R. da Silva¹ · Frank N. Crespilho¹

Received: 12 December 2022 / Revised: 26 January 2023 / Accepted: 30 January 2023
© Springer-Verlag GmbH Germany, part of Springer Nature 2023

Abstract

Since the last decade, carbon nanomaterials have had a notable impact on different fields such as bioimaging, drug delivery, artificial tissue engineering, and biosensors. This is due to their good compatibility toward a wide range of chemical to biological molecules, low toxicity, and tunable properties. Especially for biosensor technology, the characteristic features of each dimensionality of carbon-based materials may influence the performance and viability of their use. Surface area, porous network, hybridization, functionalization, synthesis route, the combination of dimensionalities, purity levels, and the mechanisms underlying carbon nanomaterial interactions influence their applications in bioanalytical chemistry. Efforts are being made to fully understand how nanomaterials can influence biological interactions, to develop commercially viable biosensors, and to gain knowledge on the biomolecular processes associated with carbon. Here, we present a comprehensive review highlighting the characteristic features of the dimensionality of carbon-based materials in biosensing.

Keywords Carbon nanomaterials · Low dimensionality · Biosensors · Graphene · Bioanalytical chemistry · Biotechnology

Abbreviations

0D	Zero-dimensional	CVD	Chemical vapor deposition
1D	One-dimensional	DA	Dopamine
2D	Two-dimensional	DNA	Deoxyribonucleic acid
3D	Three-dimensional	Dox	Doxorubicin
AuNC	Gold nanocages	ds-DNA	Double-stranded DNA
BOD	Bilirubin oxidase	FCF	Flexible carbon fibers
BSA	Bovine serum albumin	FEG-SEM	Field emission–scanning electron microscope
CDs	Carbon dots	FET	Field-effect transistor
CNDs	Carbon nanodiamonds	fM	Femtogram
CNFs	Carbon nanofiber	GFET	Graphene field effect transistor
CNHs	Nanohorns	GO	Graphite oxide
CNTs	Carbon nanotubes	GOx	Glucose oxidase
COVID-19	New coronavirus disease	GQD	Graphene quantum dots
CQD	Carbon quantum dots	Gr	Graphene
CSCNTs	Cup-stacked carbon nanotubes	HA	Hyaluronic acid
		HRP	Horseradish peroxidase
		IgG	Immunoglobulin G
		ITO	Indium tin oxide
		Lamp	Loop-mediated isothermal amplification
		LB	Langmuir–Blodgett technique
		LbL	Layer-by-layer technique
		lncRNA	Non-coding RNA
		LOD	Limit of detection
		miRNA	MicroRNA
		MWCNTs	Multiwalled carbon nanotubes

Published in the topical collection *Young Investigators in (Bio-) Analytical Chemistry 2023* with guest editors Zhi-Yuan Gu, Beatriz Jurado-Sánchez, Thomas H. Linz, Leandro Wang Hantao, Nongnoot Wongkaew, and Peng Wu.

✉ Frank N. Crespilho
frankcrespilho@iqsc.usp.br

¹ São Carlos Institute of Chemistry, University of São Paulo, Av. Trabalhador São Carlense, 400 Parque Arnold Schimidt, São Carlos, SP 13566-590, Brazil

MvBOD	<i>Myrothecium verrucaria</i> BOD
NIR	Near-infrared spectroscopy
OCP	Open circuit potential
OGB	Oxidated graphene bilayer
ORR	Oxygen reduction reaction
PEI	Polyethyleneimine
PL	Photoluminescence
pM	Picogram
PNR	Poly-neutral red
POC	Point-of-care testing device
QD	Quantum dots
RBD	Receptor-binding domain
rGO	Reduced graphene oxide
RNA	Ribonucleic acid
RT-PCR	Reverse transcription polymerase chain reaction
SEM	Scanning electron microscope
ss-DNA	Single-stranded DNA
SWNTs	Single-walled carbon nanotubes
TCVD	Monolayer graphene-based three-component vertically designed device
UV	Ultraviolet
WOR	Water oxidation reaction
XA-NSEC	X-ray absorption nanospectroelectrochemistry
XAS	X-ray absorption spectroelectrochemistry
XPS	X-ray photoelectron spectroscopy

Introduction

Diagnostic technologies represent one of the market's top sectors, especially because around 70% of medical choices are supported by diagnostic devices [1]. Depending on the application, biosensors can be constructed using proteins, whole cells, aptamers, RNA, or DNA [2, 3]. Due to these broad capabilities, carbon-based material usage in biosensors is established as successful, as seen in academic research and commercial products [3–5]. In particular, carbon-based materials can be used for the electrochemical detection of various analytes due to their distinctive electrochemical characteristics, including a broad potential window, low cost, and a negligibly small background current [6]. Additionally, the biocompatibility of carbon materials has completely transformed their potential application [7].

Carbon can form long chains of atoms, consequently exhibiting the phenomenon of polymerization. Despite having the same chemical composition, carbon atoms possess an electronic structure and atomic size that enable them to display various physical structures and distinct physical attributes; further, the fundamental standard for categorizing nanomaterials (Fig. 1) is the geometrical structure of the particles [6, 8]. The particles may include spheres and

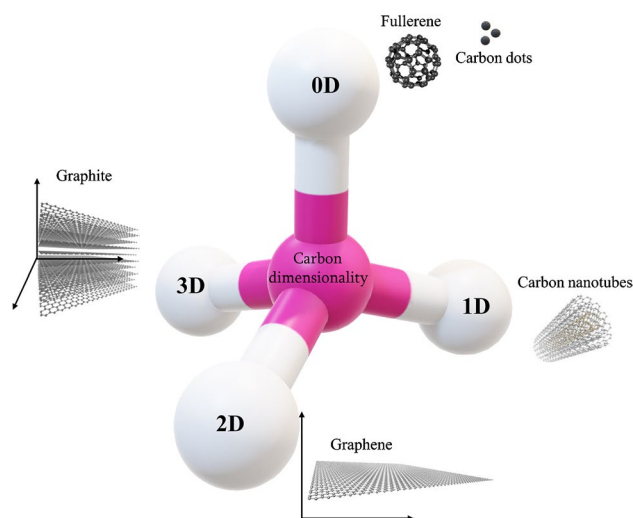


Fig. 1 Examples of 0D, 1D, 2D, and 3D carbon-based nanomaterials

ellipsoids (presented as fullerene structures), carbon nanotubes (CNTs), and nanohorns (CNHs). Allotropes of carbon, such as CNTs, graphene, fullerene, carbon dots (CDs), and carbon nanodiamonds (CNDs), are typically used in biosensing applications. Commonly, the dimensionality is classified as follows [9]: (i) zero-dimensional (0D)—including graphene quantum dots (GQD), fullerenes, and carbon quantum dots (CQD); (ii) one-dimensional (1D)—CNTs, single-walled carbon nanotubes (SWNTs), multiwalled carbon nanotubes (MWCNTs), or cup-stacked carbon nanotubes (CSCNTs); (iii) two-dimensional (2D)—graphite and graphene; (iv) three-dimensional (3D)—carbon nanofibers (CNFs), carbon sponges felt, and a myriad of composites [10]. The 2D and 1D nanomaterials are gaining popularity, laying the groundwork for a profound revolution in the flexible electronics/sensors sector [11]. Functionalization [6] and immobilization of biomolecules [3] are common for preparing carbon-based materials for biosensing/sensing purposes.

Carbon nanotechnology has already had a notable impact on different fields, such as energy storage [12], catalyst [13], energy conversion [14], electromagnetic shielding [15], bioimaging [16], drug delivery [17], artificial tissue engineering, DNA sequencing [7], and biosensors [18–23]. Efforts are underway to understand how nanomaterials can influence biological interactions [24]; further, to develop an appropriate sensor platform, integrated knowledge about carbon structure and biomolecular events is necessary. The use of carbon-based nanomaterials in biosensing is very versatile to create distinct biosensor platforms [16, 25–28], and relies on the enhanced signal and/or the immobilization of the target analyte and bioreceptor [29]. For example, biomolecule immobilization together with carbon-based nanomaterials can be obtained in undemanding experimental setups by using nanostructured films, for example, via

the layer-by-layer (LbL) and Langmuir–Blodgett (LB) techniques, providing new biosensor nanoarchitectures [30–34]. Those architectures can be diverse and provide different types of sensing platforms depending on the application [6]. However, new biosensor platforms can be designed and chosen according to the dimensionality and structural characteristics of carbon nanomaterials, which encouraged us to write the present review article. Here, we highlight the characteristic features of dimensionality of carbon-based materials in biosensing, with a focus on the literature of the last years.

0D carbon nanomaterials

The most explored examples of 0D carbon nanomaterials are quantum dots, either in the form of CQD or GQD, fullerenes, and nanodiamonds [16, 35]. GQD is considered a small piece of graphene with a length of less than 100 nm; ideally, for GQDs, a length of less than 30 nm is considered a practical benchmark size that greatly enhances quantum confinement effects [36]. An intrinsic characteristic of quantum dots is that they possess an optical absorption peak in the UV region relative to the π – π^* transition, relative to the sp^2 hybridization. The electronic spectroscopy characteristics of QDs are greatly influenced by the presence of doping elements, often nitrogen, phosphorus, and sulfur; defects, such as the alterations of C=O bonds; or surface functionalization, which lead to additional n – π^* transitions; additionally, some photoluminescence (PL) mechanistic-associated pathways are being under discussion [37].

A great extent of QD usage relies on their PL properties; GQDs showing a higher emission yield than CQDs, yet often still low, with the emission wavelength being greatly dependent on the particle size, amount of defects, functionalization types, or doping concentration, renders GQDs highly versatile and amenable for light emission tunability through bandgap engineering strategies, as represented in Fig. 2(A) [38]. The same is noticed for electroluminescence, in which the fluorescence emission results from the quantum confinement of sp^2 domains and is modulated through sp^3 defects and doping elements [39]. In GQDs, it is known that the surface functionalization associated with the delocalization of electrons and holes affects the recombination of electron–hole pairs, leading to enhanced photoemission due to decreased graphene symmetry [40]. When graphene is used in the form of GQDs, a particular practical case occurs if the material is highly oxidated, often named as graphene oxide quantum dot, with distinct spectral features and implications for QD–solvent interactions [41].

The synthetic strategies include the arc discharge of graphite, laser ablation, and electrochemical oxidation as top–down examples, and CVD, micro/nanoemulsion, microwave irradiation, and hydrothermal protocols as bottom–up

examples [39]. More recently, biological and green routes have also been explored [42]. The commonplace balance of top–down versus bottom–up approaches certainly applies here, with the former group of methodologies requiring dispersive facilities and instrumentation while enabling the rapid production of nanoparticles and allowing usage of less noble carbon sources as precursors, at the cost of limited size control. The latter requires less expensive instrumentation but often lengthy protocols, with the advantage of the controllable products' size, doping level, and overall properties, especially via the cautious selection of carbon precursors.

The surfaces of both CQDs and GQDs can be functionalized through a myriad of strategies, either simple physisorption or via exploring reactions, such as amide coupling, coupling streptavidin–biotin for affinity binding [43], and even click-chemistry [44]. Zero-dimensional carbon nanomaterials have a wide range of applications in bioanalysis literature, especially driven by the thrilling advances in liquid biopsy and point of care [45, 46], owing to their photoluminescence and electroluminescence properties, which makes these materials unique compared to 2D or 3D carbon nanomaterials, or via electrochemical approaches. Additionally, readers can find examples and future expectations concerning the use of 0D carbon nanomaterials in recent reviews [16, 47]. Here, some frontier applications associated with biosensing and bioimaging are highlighted as they represent some of the major advances in using CQDs and GQDs for bioanalysis.

The optical features of both CQDs and GQDs show exciting versatility for their practical usage, as the wavelength of their maximum photoluminescence can be easily tuned via the introduction of distinct groups at the edges of the material and modulating the bandgap and producing redshifts of up to 200 nm either by inducing the formation of an additional π character or by creating n -orbitals to the structure, as exemplified (Fig. 2(A)) [38].

In electrochemistry-based biosensors, the use of CQDs has found success in improving the early detection of biomarkers for life-threatening conditions, such as myocardial infarction and heart failure, which are often detected or monitored through biomarkers such as troponin-I and troponin-T, creatine kinase, and myoglobin. A screen-printed electrode decorated with graphene quantum dots and gold nanoparticles, followed by anti-cardiac troponin-I, was recently developed [50]. The electrochemical analyses were performed using human serum, providing quantitative results in ca. 10 min with square-wave voltammetry, until concentrations as low as 0.5 pg mL^{-1} . In a similar context, a study explored the photoelectrochemical sensing of troponin-I using a modified electrode capable of generating a large variation in photocurrent and charge-transfer impedance via antigen–antibody interactions [51]. Zinc stannate (Zn_2SnO_4) cubes were deposited onto an indium–tin oxide

(ITO) glass conducting electrode, followed by subsequent modification with N,S-GQDs and CdS, employed to co-sensitize the cubic particles, narrow down the bandgap, and enhance the photoelectric properties of zinc stannate. Using this approach, troponin-I concentrations as low as 0.3 pg mL^{-1} were detected in serum.

In electrochemical experiments, it is very important to consider the complexity of the samples, which frequently translates to the requirement of the anti-fouling ability of the biosensor surface. As an example, a research engendered a sensing platform comprising of vertically ordered mesoporous silica–nanochannel film, with channels $< 5 \text{ nm}$ in size perpendicular to the underlying gold electrode, resulting in an anti-biofouling ability [48]. The nanochannel platform was modified with OH⁻ and NH₂–GQDs through electrophoresis, as shown in Fig. 2(B), to act as a recognition element or signal amplifier. Their GQD-based platform enabled the detection of Hg²⁺, Cd²⁺, Cu²⁺, and dopamine through differential pulse voltammetry in complex samples such as seafood, soil-leaching mixtures, and serum, achieving quantification in the pM to nM range. This approach complements the widely reported sensing of heavy metals due to their affinity to functionalized GQDs (affinities of HO-GQDs for Hg²⁺ and Cd²⁺ for H₂N-GQDs), therefore inducing a fluorescence quenching optical effect; in complex samples, however, the selectivity of these photoluminescence quenching approaches is a challenge.

In another example, GQDs were employed as substrates for horseradish peroxidase (HRP) to provide an amplified electrochemical signal for the biosensing of a specific miRNA chain, accompanied by a change in the color of the solution [52]. The GQD-based miRNA enzymatic biosensor platform was used to analyze human serum samples and achieved the detection of the analyte in the fM to pM range. The detection of miRNA was recently explored, designing a biosensing platform for the quantification of a specific pancreatic cancer–derived miRNA, expressed as pre-miR-132, based on the fluorescence variation of N-doped GQDs when bound to a bait ss-DNA sequence or the bait-target assemble, in a likely charge-transfer event [53]. The minimal concentration in the micromolar range indicates that these important biomarker sensors possess the potential for achieving ultrasensitive detection. It must be highlighted that despite the interesting electrochemical properties of CQDs and GQDs, the optical features of these materials, especially their photoluminescence, are pivotal properties that make them unique, compared to commonplace carbon nanomaterials with higher dimensionality. For this reason, the PL of carbon-based nanomaterials is often explored in the bioimaging field.

As a clear example of CQD usage as a fluorescent nanoprobe, a research developed an assembly of polyethyleneimine (PEI)–modified CQDs (P-CD) and hyaluronic

acid–conjugated doxorubicin (Dox, a chemotherapy drug), which show only weak photoluminescence emissions in the normal cellular environment (NIH-3T3) [49]. In the aforementioned study, the authors explored the high affinity of hyaluronic acid (HA) to CD44 receptors, which are overexpressed on the membranes of several cancer cells. HA is cleaved by hyaluronidases after endocytosis; further, it is commonly more abundant in cancer cells. Hence, the P-CD/HA-Dox probe is easily absorbed by cancer cells, and after cleavage of HA-Dox, the fluorescence of P-CDs is restored, and the cells become optically identifiable (Fig. 2(C)). Additionally, as Dox is then cleaved from HA, it can intercalate with DNA pairs and inhibit efficient replication; therefore, these probes acted as both bioimaging and drug-delivery probes.

For additional examples of CQDs and GQDs applied to biosensing and bioimaging, especially for circulating nucleic acid bioanalysis, the readers can refer to the selected literature [54, 55]. Although we highlighted quantum dots, applications of fullerenes can be found in literature as photoactive materials bound to dyes, such as methylene blue [56], and as a charge-transfer mediator, especially for nucleic acid sensing [57, 58]. Nanodiamonds represent the other class of 0D-carbon nanomaterials of interest, showing high biocompatibility, the typical chemical inertness of diamonds, a high surface area, the possibility to functionalize surface regions (as in –NH₂ and –COOH-terminated nanodiamonds), and the ability to be used for drug delivery and bioimaging, especially with tailored structure defects that drive photoluminescence [59].

1D carbon nanomaterials

The group of 1D carbon-based nanomaterials commonly explores carbon nanofibers and carbon nanotubes, either in the form of a single cylindrical graphitic sp²-hybridized carbon network denominated single-walled carbon nanotube (SWCNT), or in the form of concentric multiple cylindrical structures, in the so-called multiwalled carbon nanotubes (MWCNT); other less common presentations are also possible, such as the cup-stacked carbon nanotubes (CSCNT), with higher edge content and, therefore, oxidized functional groups, with crucial consequences to electrostatic interactions and charge transfer [26]. These nanomaterials can be produced by arc discharge and laser ablation [60], but catalytic chemical vapor deposition is a classic and very efficient method of producing nanotubes of a wide range of diameters and lengths, with good helicity control—although still a challenge—due to the initial hemispherical pentagon cap formation, driving, and defining the elongation of the CNTs [26]. In these materials, the optical and chemical properties are greatly affected by the doping—either electron donors or acceptors [61], and some methods have been shown to promote controllable doping [62]. Structural topological and

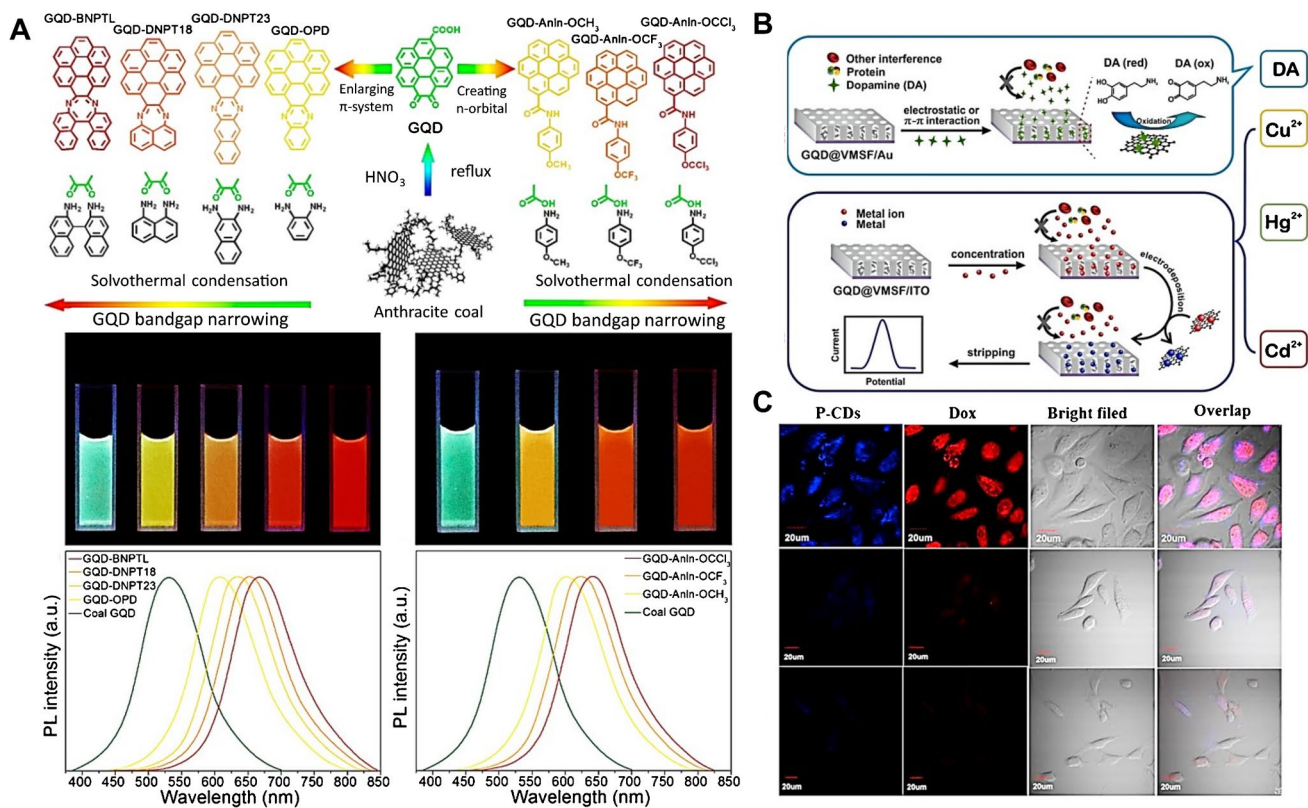


Fig. 2 (A) (Top) Schematic representation of the tuneable photoluminescence redshift caused by the introduction of n-orbitals or by the enlargement of π -systems in GQDs, with their photographs under a UV lamp (middle) and the respective spectra (bottom). Reproduced from [38] with permission from the American Chemical Society. (B) Incorporation of GQDs into a mesoporous silica-nanochannel film through electrophoresis, resulting in anti-fouling properties for the electrochemical sensing of Hg^{2+} , Cd^{2+} , Cu^{2+} , and dopamine (DA) in complex samples, such as food, soil, and serum.

Reproduced (adapted) from [48], with permission from the American Chemical Society. (C) Bioimaging of HeLa cancer cells based on the fluorescence of CQDs after endocytosis due to preferential hyaluronic acid-CD44 interactions compared to normal cells, in blue and red channels, and the corresponding bright field (first row); HeLa cancer cells pre-treated with hyaluronic acid, showing weak PL (middle row), and non-cancer NIH-3T3 cells indicating weak PL (bottom row). Reproduced from [49], with permission from Elsevier

incomplete bonding defects, such as vacancies, pentagons, and heptagons disrupt carbon hexagons' regularity and, therefore, cause important electronic charge localization and produce changes to the density of states [63].

When it comes to CNT properties, the regularity of the structure as a rolled-up graphene sheet promotes high conductivity in the length axis, thermal stability, and mechanical resistance, leading to a wide presence of these materials in bioanalytical devices, most often as electrical conductivity enhancers for transduction [18]. While MWCNTs behave as metallic conductors, SWCNTs are more versatile as a semi-conducting characteristic can also be obtained depending on the diameter and helicity control, and the present bandgap in this case is responsible for near-infrared fluorescence emission [64]. The anisotropy relative to the edge regions, with a higher amount of oxidized groups, also provides a central role in electron transfer and electrocatalysis [65]. Additionally, as commonplace routes for CNT production employ metallic precursors, researchers should be extremely careful

about metallic impurities which can promote catalytic artifacts and undesired contamination in biological environments [66].

In terms of 1D carbon-based material applications in bio-analytical devices, there is a wide range of well-succeeded examples in literature, mostly for biomarker sensing and cell bioimaging, with recent interests boosted by the point-of-care (POC) development trend and the exciting research pathway toward ultrasensitive biosensing for liquid biopsy. In this context, an ultrasensitive and selective biosensor was developed for quantifying breast cancer exosomal miRNA21 [67]. For this, the authors employed CNTs as the channel material in a field-effect transistor (FET), as in Fig. 3(A), with subsequent incorporation of gold nanoparticles onto which a thiolated DNA probe is chemically linked as the recognition element. The hybridization of the miRNA leads to a current change in the CNT-FET device, and authors reached an attomolar limit of detection, with satisfactory performance in clinical samples.

A p-type CNT-FET strategy was also employed for the fast detection of the SARS-CoV-2 surface spike protein S1, employing CNTs as charge-transfer transducers and relying on anti-SARS-CoV-2 S1 antibodies to grant selectivity to the protein [68]. The variation of current induced by the antigen–antibody coupling in the affinity sensor in the case of a positive response was evaluated in fortified saliva, and the platform was able to achieve a limit of detection of 4.12 fg mL^{-1} .

In the context of POC bioanalytical development, CNT-FETs are also showing important advances to allow the early diagnosis of health conditions, such as through blood biomarkers, which brings the additional challenge of low biomarker concentration and high protein concentration that promotes surface biofouling [45, 69]. A CNT-FET biosensor for the β -amyloid, using aptamers as the recognition element in the affinity sensor and 6-mercapto-1-hexanol, tween 20, and bovine serum albumin (BSA) for anti-biofouling, was proposed [69]. The sensor delivered high selectivity ratios for two tested amyloid peptides and a limit of detection in the attomolar range.

The usage of MWCNTs as electroactive materials for the anchoring of metallic nanoparticles and biorecognition elements is also being frequently explored [74–76]. In recent work, the detection of a long non-coding RNA (lncRNA), a molecule with regulatory roles and with an increased circulating concentration in conditions such as lung adenocarcinoma, was performed by the engineering of a disposable electrode strip based on amidated MWCNTs as a conducting supporting element for the incorporation of gold nanocages (AuNC) and a specific probe DNA (Fig. 3(B)) [70]. The recognition of the target DNA in this affinity sensing platform promotes a current variation and limit of detection in the femtomolar range, with good results in human serum samples.

When it comes to exploring bioanalytical imaging, carbon nanotubes have been employed with success with multiple distinct strategies. A single-chirality SWCNT probe was used for biosensing due to their optical properties as NIR bands and Förster resonance energy transfer (FRET), developing a set of functionalized CNTs coated with helical polycarbodiimide polymers with distinct functionalities [71]. By differential interaction of each functionalized SWCNT with sub-cellular structures, the authors were able to observe internanotube FRET and image separate parts of the cell, such as the nuclear and cytosolic regions (Fig. 3(C)). This work emphasizes the exciting room for CNT-based FRET nanoprobe for multiplexing sub-cellular bioimaging. SWCNT uptake via cell membrane transport is still not explored as needed, and recent works acquired important pieces of information regarding the role of CNT length and surface charge for uptake in prokaryote cyanobacteria for fluorescence imaging [77]. Also, it was elaborated a CNT-based biosensing platform for circulating tumor cells (CTCs) in

an antigen-independent capture fashion, where the preferential attachment of CTCs to a CNT-decorated surface is advantageously explored (Fig. 3(D)) [72]. In this kind of platform, the absence of antigen dependence enables the isolation of distinct CTC phenotypes and imaging without major disturbances of microfluidic devices, as no transfer is needed for microscopy analyses. The ingenious platform enabled the capture of multiple breast cancer phenotype CTCs from the same patient and offers a high impact for future studies of metastasis evolution, dynamics, and therapeutic selection with observations at a single-cell level.

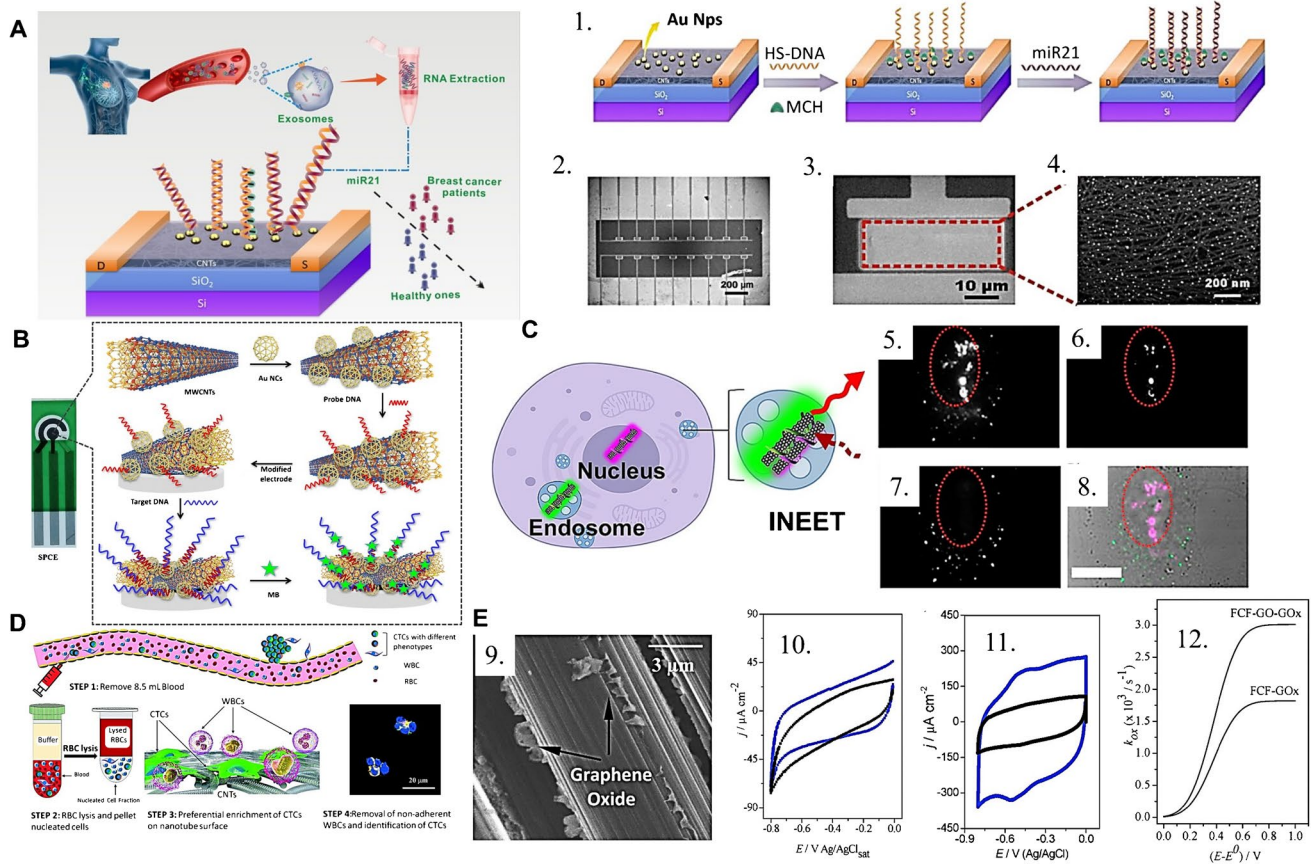
1D materials such as flexible carbon fiber can also be explored combined with other carbon nanomaterials such as graphene oxide (a 2D material) to enhance the electron-transfer process in enzymes as glucose oxidase, as represented in Fig. 3(E), with a decreased activation energy of the process and a shorter distance to the electrode [73].

2D carbon nanomaterials

Graphene has attracted great attention with regard to biosensing platforms. It is considered a two-dimensional nanomaterial with outstanding electronic properties that are widely envisioned in analytical and bioanalytical applications [78, 79]; herein, we refer to graphene as a single sp^2 -hybridized layer of carbon atoms, in its monolayer or isolated form [8, 80]. When in its isolated form, whether obtained from mechanical exfoliation [81] or chemical vapor deposition (CVD) [82, 83] process, graphene is characterized by its unique structural, electronic, and interfacial properties at the basal plane [84], isolated graphene edge [85–87], and an edge periphery [88, 89]. Graphene can also be easily handled, given its high surface area and suitable physical properties [90], in some cases, in its single-crystal form [91, 92]; further, it is a promisor candidate for use in the fabrication of bioelectronic devices due to its high carrier mobility [93], physical stability and the ease of modifying its chemical characteristics [94], and characteristics of electro-transfer depending on functionalization and modification [73, 95], which can be achieved by oxidative or non-oxidative experimental protocols [96, 97].

There are still many difficulties associated with graphene use, for example, when reproducible sizes of single sheets or surface contamination from the fabrication process hamper its practical applications [98–100]; chemical or electrochemical (*e-etching*) [101, 102] protocols were reported in the last years as methods to overcome such limitations. In addition, for the miniaturization of devices, it is crucial to examine edge effects in the diffusion mechanism of electroactive species in low-dimensional electrodes [103].

With regard to the development of graphene-based bioelectronics, there is much progress in the biosensing



of metabolites, to the understanding of the interactions of graphene with peptides [104], DNA [105], or neurotransmitters [106]. Bioanalytical measurements are traditionally performed *in vitro* or *in vivo* [107], using body fluids [108], via the design and integration of electronic devices on the body or the implantation of the devices into living tissues [109]. Interfacing electronics with tissues for bioanalysis has been an area of interest for decades, but many of these devices involve the use of rigid and bulky substrates with robust physical connections; this can make the acquisition of experimental data more difficult, since mechanical properties may influence the signal captured [110]. These

spectral analysis. Reprinted (adapted) from [71], with permission from the American Chemical Society. (D) Operational schematic for the CNT-based antigen-independent capture of circulating tumor cells in human blood serum, exploiting the preferential interaction of CTCs to CNTs and enabling the observation of multiple phenotypes of breast cancer cells. Reproduced from [72] with permission from the Royal Society of Chemistry. (E) (9) FEG-SEM image of the flexible carbon fibers with graphene oxide exfoliated directly onto the filaments' surface, (10) cyclic voltammograms of FCF and FCF-GO and (11) FCF-GOx and FCF-GO-GOx in sodium phosphate buffer, (12) oxidative electron-transfer rate constant as a function of the overpotential for FCF-GOx and FCF-GO-GOx. Reproduced from [73], with permission from the Royal Society of Chemistry

physical characteristics limit the integration of such electronic devices in soft or curvilinear surfaces, such as human skin or brain tissues; hence, the discovery of graphene emerged as a versatile and promisor material for the future fabrication of biomedical devices in the future [110].

Another example is the regular monitoring of glucose which involves the conventional measurement of its levels in blood via invasive finger-stick procedures, which are substituted by using temporary implantable microneedles or monitoring glucose levels in saliva, tears, or sweat. As a more reliable material for measuring the levels of glucose in body fluids, owing to its high specificity and low selectivity for

detection, large-area graphene has been recently shown as a non-invasive and promising material. The development of a graphene-based sensor with thermoresponsive microneedles for diabetes monitoring in human skin is reported [108]. Large-area graphene is also a very versatile material and has been reported as a promising platform to detect neuronal activity in the brain. Also, it is reported [106] that single-layer graphene increases neuronal firing by tuning the distribution of extracellular ions at the neuronal interface.

The detection, manipulation, and sequencing of single DNA molecules are both scientifically and commercially relevant. As an example, a study [111] reported the fabrication of nanopores onto single and suspended graphene ribbons to detect the translocation of single DNA molecules. In this case, the simultaneous ionic and electrical current of graphene was recorded when DNA molecules flow through an isolated graphene nanopore (single event or translocation of DNA). As other examples of ultimate advances in graphene-based technology, graphene has been investigated for its use in electrical–electrochemical point-of-care devices, DNA sensing, and electrical–electrochemical sensing devices (Fig. 4).

The development of novel technologies for the detection of bacteria [112] or viruses [113] is of great importance to our society. The early diagnosis of emerging pathogens is very critical for human health. With respect to the COVID-19 pandemic, graphene has also shown powerful potential for the development of hybrid electrical electrochemical devices [114]. The importance of such protocols for early detection can be substantiated by their specificity and speed of detection compared to those of the conventional molecular RT-PCR methods [115, 116]. For instance, graphene was reported as a powerful miniaturized platform for the development of POC serologic COVID-19 diagnosis (Fig. 4(A)), with an analysis time of up to 15 min [113]. The application of an electrical–electrochemical vertical device (EEVD) was proposed, based on hybrid electrical and electrochemical working principles [113]. Different from a G-FET, it utilized a hybrid system operating under a quasi-circuited mode and comprising a Ag/AgCl/Cl electrode as the gate. This innovation produces 10× more signal when compared to a traditional G-FET. Figure 4(B) shows the EE I_{ds} vs. V_{ds} curves that were acquired within a potential range with no faradaic process, considering the bare graphene and all following modification onto its surface. Fig. 4(C) shows the wide linear dynamic range of IgG concentrations varying from 10^{-12} to 10^{-7} g mL⁻¹, and Fig. 4(D) shows the distribution of OCP displacement values for $n=9$ for positive and negative IgG detections in diluted patient serum samples by G-PNRAuNP/RBD EEVD. This is clearly exemplifying that graphene technologies could be adapted for use in other emerging bioanalytical strategies for controlling pandemic diseases with a high probability of success.

Monolayer graphene-based three-component vertically designed device (TCVD) has also been used as a

biosensing platform for DNA, either by ds-DNA adsorption onto graphene or DNA hybridization from the bulk solution (Fig. 4(E)). Interestingly, the interface properties of the device change according to the characteristics of the components used and can be adjusted due to its versatility. For example, the absence of a semicircle in the EIS spectra and the Nyquist plots indicates a diffusive response for the graphene monolayer deposited onto the gold (Au) electrode. From the Nyquist plots, the characteristic linear lines indicate the absence of charge transfer, as well as the diffusive response for the pristine graphene on the Au electrode (Fig. 4(F, I); black curve). The electrochemical impedance response changes either for the adsorption of ferrocene (Fc) or ds-DNA (concentration of $0.2 \mu\text{mol L}^{-1}$). The total interfacial capacitance values of the graphene monolayer electrodes in the presence or absence of ds-DNA are shown in Fig. 4(G, H and J, K, respectively), and were acquired from the simulation of the equivalent circuit.

Graphene monolayers show a high sensitivity to any change on the surface and can be monitored by measuring the capacitance of the electrodes. In this case, the TCVD ($C=2.5 \pm 0.08 \mu\text{F cm}^{-2}$) showed a higher decrease in the capacitance after Fc adsorbed onto the surface of the graphene monolayer ($C=1.6 \pm 0.06 \mu\text{F cm}^{-2}$, $C=2.4 \pm 0.10 \mu\text{F cm}^{-2}$, respectively), and a threefold higher sensitivity for detecting ds- than biosensors in which graphene monolayers deposited onto Si/SiO₂ substrates. EEVDs have also been reported to be constructed via the combination of horizontally aligned graphene–ferrocene heterojunctions as a powerful electrode configuration for DNA sensing. The EEVD was composed using two working and auxiliary electrodes in a short-circuit configuration and compared with the field-effect conventional device (Fig. 4(M)). The quantification of ss-DNA with EEVD graphene–Fc devices that were able to reach an LOD of 5×10^{-21} mol L⁻¹ for the detection of ss-DNA is shown in Fig. 4(N).

Beyond the graphene monolayer, bilayer-based devices have been proposed as a new strategic design of biosensors and its fundamental study on the atomic behavior of defects and stacking layers of oxidated graphene bilayer (OGB) provides devices with superior electrochemical performance, when compared to pristine graphene electrodes [118]. The electrochemical impedance spectroscopic study showed that the charge transfer of the OGB electrodes improved by 90% as a result of the existence of edge-like defects 100 times greater than those of pristine electrodes. Attributable to the superior electrochemical activity of the OGB electrode and conciliating the surface modification on the upper layer with exceptional electron transport of the bottom layer (that remained intact), this study provided a new insight into the superior electrochemical properties of OGB electrodes, making it a potential electrode for application on-chip devices. Additionally, the presence of high-oxygen content has been

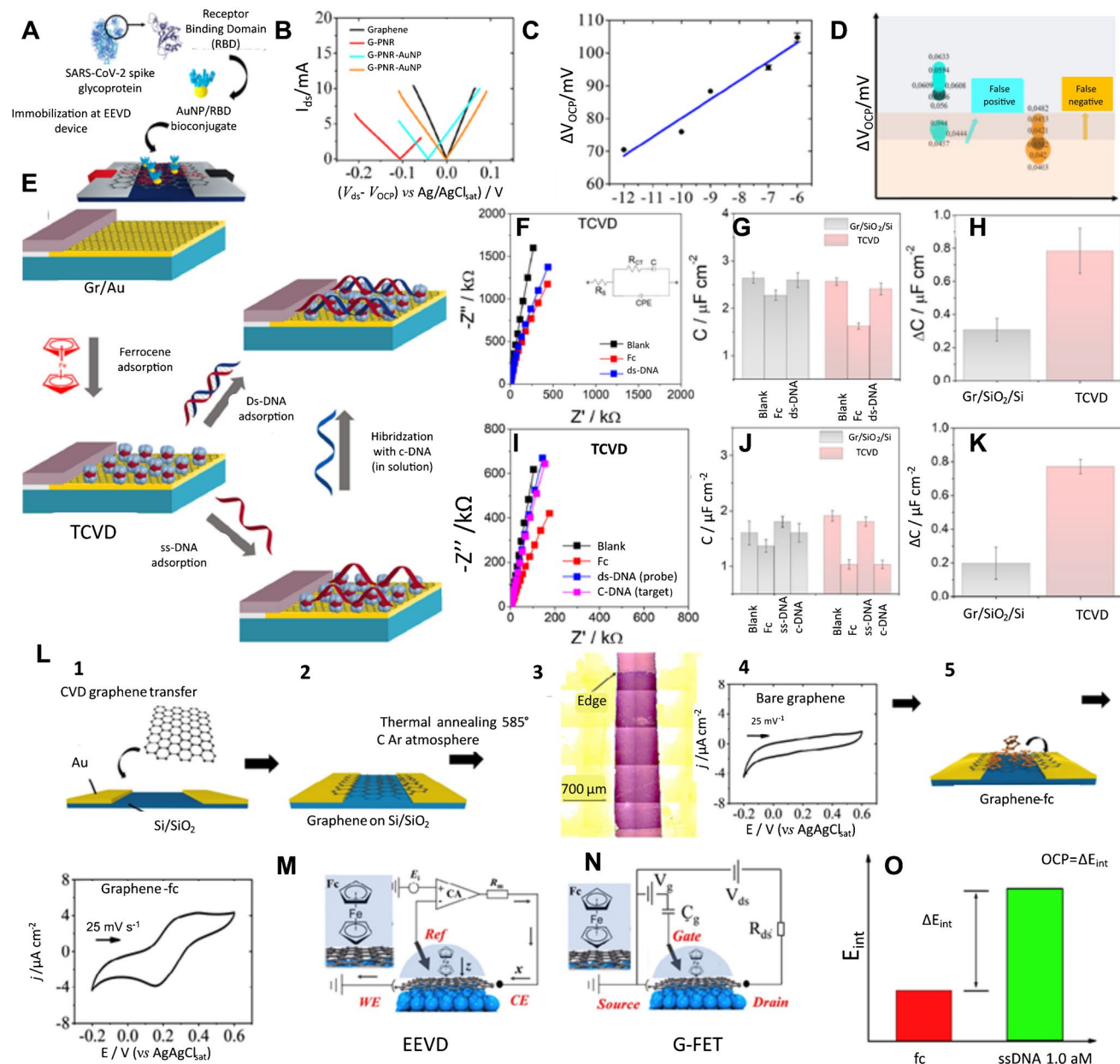


Fig. 4 Graphene-based bioelectronics. (A) Schematic representation of the method for immobilizing AuNP/RBD onto G-PNR. (B) Hybrid I_{ds} vs. V_{ds} EE curves for bare graphene (black), G-PNR (red), G-PNR-AuNP/RBD (cyan), and G-PNR-AuNP/RBD after interactions with human IgG (orange) in PBS buffer. (C) Calibration curve for IgG detections from 1.0 pg mL^{-1} to $1.0 \text{ } \mu\text{g mL}^{-1}$ in PBS as support electrolyte by hybrid I_{ds} vs. V_{ds} EE experiments. (D) Distribution of OCP displacement values positive and negative IgG detections in diluted patient serum samples by G-PNRAuNP/RBD EEVD. Reproduced from [5], with permission from Elsevier. Monolayer graphene-based three-component vertically designed (TCVD) device. (E) Schematic illustration of the detection of ds-DNA adsorption and hybridization in solution using the TCVD device. (F) Nyquist plots obtained during the adsorption of Fc and ds-DNA onto the device surface. (G) Plot of the measured capacitance of the TCVD and Gr/SiO₂/Si electrode fitting the Nyquist plots to the equivalent circuit (inset of F). (H) Plot of the change in the capacitance after the hybridization of the DNA on the electrode surface. (I) Nyquist plots of the TCVD electrode obtained during the adsorption of Fc, ss-DNA, and

complementary DNA to the electrode surface. (J) Plot of the measured capacitance of the TCVD and Gr/SiO₂/Si electrode obtained from fitting the Nyquist plots to the equivalent circuit (inset of J). (K) Plot of change in the capacitance after the hybridization of the DNA on the electrode surface from the solution. Reproduced from [117], with permission from Elsevier. (L) Electrical–electrochemical vertical device (EEVD) device preparation description. Steps 1 and 2 correspond to graphene wet transfer methodology. Step 3 presents an optical micrograph of graphene on SiO₂/Si. Step 4 depicts an electrochemical response of typical pristine graphene. Step 5 illustrates ferrocene in ethanol drop casting and its adsorption onto graphene, forming a graphene-fc vdW heterojunction. Step 6 illustrates a typical final cyclic voltammogram obtained for graphene-fc in phosphate buffer solution. (M) Schematic representation of the working principles of an EEVD with the proposed graphene-fc heterojunction. (N) Schematic representation of a GFET’s working principles for comparison with M. (O) Representation of ss-DNA quantification using EEVD graphene-fc devices. Reproduced from [113], with permission from Elsevier

shown to affect molecule adsorption, including eventually hindering the process [119].

3D carbon nanomaterials

The class of 3D carbon-based materials can be regarded as a network of lower-dimensional structural elements, such as carbon felts comprising carbon fibers [120], carbon nanotube weaves [121], graphene-based composites [122, 123], and combined hierarchical materials [124, 125]. These carbon materials can be presented as stand-alone matrices or combined with other materials as a multitude of polymers and biopolymers, gels, metallic particles, and oxides. Among the advantages of 3D carbon-based materials is their capability to offer a high surface area for the adsorption and immobilization of biomolecules, practical manipulation for the construction of biosensing platforms, and versatility, regarding both chemical functionalization and mechanical properties. Here, we will highlight some studies using different platforms to produce nanoblister for flexible biosensors, wearable biosensors, and porous and mesoporous structures to provide a relevant increase in both sensitivity and molecular recognition.

As the orientation of adsorbed redox-active enzymes onto electrodes deeply affects the electron transfer from the enzyme's active center to the electrode, a research employed a carbon fiber matrix decorated with reduced graphene oxide (rGO) as inter-fiber sheets and cup-stacked carbon nanotubes (CSCNTs) coating the fibers' surface, as seen in Fig. 5(A), enabling favorable surface-enzyme interaction, efficient electron transport, and high accessibility to the active sites to drive effective electrochemical communication [120]. This platform was employed to study glucose oxidase (GOx) as a model redox enzyme, and the results indicated that not only does a kinetic improvement depend on the presence of rGO and CSCNT combined, that is, a 3D composite, but also that a considerable conformational change of GOx is evident when it is adsorbed onto the modified felt electrode, which exposes its active center at the same time, compromising the biocatalytic activity.

Flexible carbon fibers can also be applied to produce carbon-based nanoblister, as represented in Fig. 5(B). Nanoblister can improve the electrocatalytic processes for high-performance glucose dehydrogenase [126]. When it comes to wearable devices, carbon nanotubes have been employed combined with hydrogels to construct conducting, adhesive, and mechanically resistant stretchable materials for sensing. A study exploited the remarkable conductivity of CNTs modified with polydopamine in a composite with agarose hydrogel and glycerol (Fig. 5(C)) [127]. The composite presented humidity retention, skin biocompatibility, and thermal stability across a wide temperature range, underscoring its promising applicability for use in skin-based wearable biosensors.

3D carbon-based nanomaterials can also be employed for coupled technique studies [117, 118], such as the study of the oxygen reduction reaction process by bilirubin oxidase (BOD) using in situ X-ray absorption spectroelectrochemistry. Mesoporous 3D carbon nanoparticles can form matrices, as in Fig. 5(D), and maximize BOD loading while maintaining high electronic conductivity.

The production of 3D hierarchical and structured platforms with carbon nanomaterials is another exciting possibility, especially when combined with smart materials, such as thermoresponsive polymers. A multilayered porous graphene oxide coating onto ITO electrodes was proposed using the breath-figure method [129]; the porous graphene oxide surface inside and outside the pores was then locally functionalized with brushes of poly(N-isopropylacrylamide), a thermoresponsive polymer, generating a platform that blocks the access of species from the external medium to the electrode at room temperature, while enabling the access of these species to the electrode after heating; this, in turn, causes the reversible contraction of the polymeric brushes and the opening of the pores, reversibly (Fig. 5(E)). This 3D carbon-based thermoresponsive physical gate platform opens the room for smart chemical sensors that are self-activated through external stimuli, such as body temperature, and can be extrapolated to light, pressure, and chemical activation.

A similar rationale can be obtained using a glassy carbon electrode decorated with MWCNTs to improve enzyme immobilization and communication [128]. In their work, a carbon cloth loaded with carbon nanoparticles was employed to maximize BOD loading while maintaining high electronic conductivity. A similar rationale was explored elsewhere [130], using a glassy carbon electrode decorated with MWCNTs, BOD and Nafion for acquiring XAS data for water oxidation reaction (WOR) in multiple steady-state electrochemical potentials (Fig. 5(F)).

Additionally, mesoporous structures of electrodes applied with different in situ analytical techniques facilitate the in-depth study of interface elements and signal transduction and provide relevant information for the fabrication of more sensitive and stable biosensors. The combination of carbon nanomaterials has been a new trend to support, mainly, new configurations of biosensors operating under either direct or mediated bioelectrocatalysis [131–133].

Challenges and perspectives

With regard to commercial prospects, it is reported that the carbon material market is segmented as follows: MWCNTs, CNTs, other categories, and end-user industries (electronics, healthcare, energy, aerospace and defense, automotive) [134, 135], and its global market is projected to reach almost \$32.8 billion by 2030 [135]. Although these numbers involve the utilization

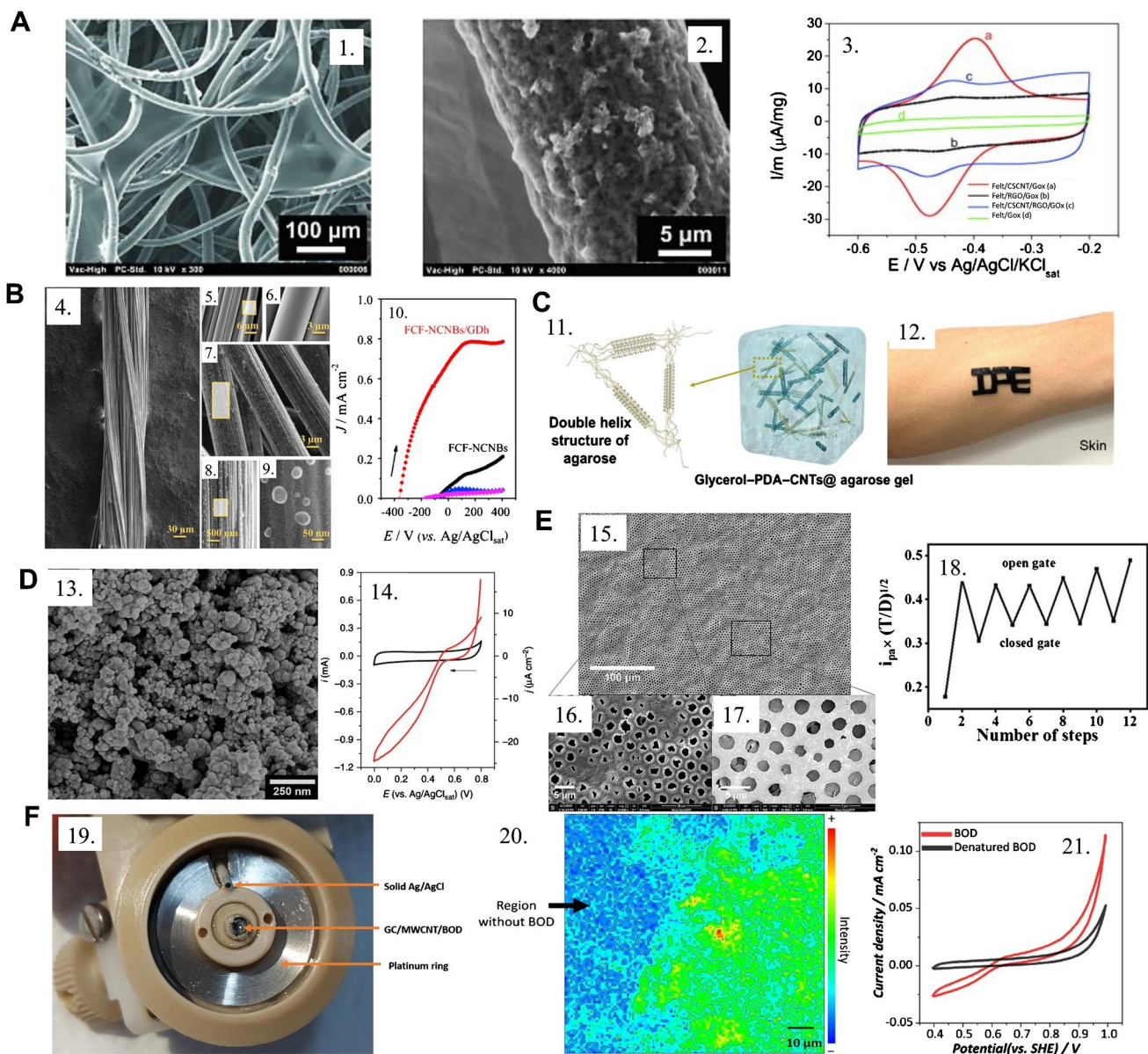


Fig. 5 (A) Scanning electron microscopy images of (1) felt/CSCNTs/graphene oxide material, (2) felt/CSCNTs/graphene oxide image at higher magnification, and (3) CSCNT/RGO-coated fibers and the corresponding voltammograms in the presence of immobilized GOx in 20 mmol L^{-1} PBS and 0.1 mol L^{-1} KCl. Reproduced from [120], with permission from Elsevier. (B) (4–9) Micrographs of carbon fibers and carbon nanoblister generated through chemical processing and (10) the electrochemical response to glucose. Reprinted (adapted) from [126], with permission from Elsevier. (C) (11) Fabrication and mechanical tests of a 3D CNT-agarose hydrogel composite for (12) application in skin-based wearable biosensors. Reprinted (adapted) from [127] with permission from the American Chemical Society. (D) (13) SEM micrographs of the mesoporous carbon matrix with high carbon nanoparticle loading employed as the working electrode for BOD immobilization, (14) cyclic voltammogram of *MvBOD*-modified electrode in

(red line) O_2 -saturated electrolyte performing the ORR and (black line) Ar saturated demonstrating no process for the bioelectrocatalysis of ORR. Reprinted (adapted) from [128], with permission from *Nature*. (E) (15–17) SEM micrograph of a graphene oxide/poly(N-isopropylacrylamide) porous formed after a polymerization time with the (18) electrochemical signals from redox probes in the external medium before and after sequential thermal opening of the polymeric brushes gate, operating in a smart-sensing thermal stimulus-activated electrochemical sensor. Reprinted (adapted) from [129], with permission from the American Chemical Society. (F) (19) A MWCNT-based bioelectrode for BOD immobilization to a XAS-analysis assembly; (20) a chemical Cu K-edge XA-NSEC mapping onto a MWCNT/BOD/Nafion bioelectrode, enabling the localization of high enzymatic loading; (21) biocatalytic water oxidation reaction obtained with the MWCNT/BOD/Nafion bioelectrode. Reprinted (adapted) from [130], with permission from Wiley

of carbon-based materials in the automotive industry, healthcare represents a critical area of focus for these materials, given that they can be used for assessing medication-associated aspects, e.g., tissue imaging. MWCNTs are the principal material of the carbon nanotube market, particularly for clinical applications [135]. There are many possibilities contained in the properties of carbon-based materials discovered so far. However, additional adjustments/revisions or even modifications for commercial-level applications are necessary, especially when aiming at the production of biosensing platforms.

Among the main perspectives, one can secure that the future of carbon nanomaterials will roam through the pursuit of new technologies, applications, and also the assurance of safe handling and in vivo safety, based on current research [136]. Recently, discussions concerning CNT safety and pressure for restricted usage have been presented, including the addition to the Substitute It Now (SIN) List by ChemSec, in a decision taken after reports indicating potential carcinogenicity, reproductive deleterious effects, and additional long-term health damage in in vitro and mice studies [137]. An immediate response by multiple researchers was issued, with a worry that an unclear depiction of the facts would hinder relevant advances and safe usage of CNTs [138]. It is clear that the risk assessment of a wide class of materials with an immense presentation variation as CNTs is an extremely difficult task, and reports from other agencies emphasize the importance of avoiding the absorption of long, aggregated, and concentrated CNTs with metallic particles as remaining impurities from catalytic production. The data heterogeneity in toxicity studies implies that CNT concerns should be narrowed down to specific ranges of length, diameter, concentration, aggregation, and purity.

Concerning the applications, the purity, form, presence of heteroatoms, and oxidation levels have a notable impact on carbon-based biosensor performance, since these factors frequently affect electrical conductivity, binding interactions between the surface and biomolecules, and the ability of biomolecules to adsorb onto the biosensor surface. Additionally, to construct biological sensors, it is crucial to evaluate the overall design concept, production techniques, and real-world application based on these materials. There are numerous scientific publications using the keywords “carbon-based sensors” and “carbon-based biosensors,” with most of them being original research articles. Certainly, modern-tech advances, such as portable, flexible, and wearable devices, are relevant for a multitude of applications. However, only a minority are currently commercially available. Although many biosensors show promise for a variety of technological and scientific applications, they are associated with several challenges in terms of mobility, selectivity, sensitivity, and multi-analyte detection in commercial fields. To overcome these challenges, the devices need to be low cost and suitable for large-scale production; demonstrate rapid, robust, and

efficient performance; and achieve quick data acquisition and transmission, which will aid the construction of databases to monitor a specific disease or target analyte.

Regarding carbon-based materials, an expansion of novel carbon forms, especially in academic fields, including new precursors, especially those obtained via sustainable methods, such as the use of biomass, and the combination of different hybridization states (sp, sp², and sp³), synthesis routes, functionalization, heteroatoms, or even new carbon forms, is expected. All these improvements are closely related to our interdisciplinary knowledge; innovation in technologies can lead us into a new era of the transformation and synthesis of materials, especially aiming at the ecofriendly manufacturing process for these materials. Additionally, it is important to mention that to achieve this goal, theoretical studies are needed, given their valuable contribution to predicting the structures, electron mobility, functionality, and reactivity of carbon surfaces. The functionalization of carbon-based materials is also an upcoming trend, since it provides the ability to customize the chemistry of the surface required for a specific application. It is worth mentioning that the standardization of the biomolecule immobilization procedure is a notable challenge that can affect the interactions of the target biomolecules with the carbon-based material. Synthesis methods that combine different carbon-based materials with dimensionalities are not a simple task, and achieving this goal could represent a breakthrough as it could simplify the construction of miniaturized devices.

Acknowledgements We gratefully acknowledge the support of the Coordinating Agency for Advanced Training of Graduate Personnel (CAPES), MeDiCo Network CAPES-Brazil, grant number: 88881.504532/2020-01; National Council of Scientific and Technological Development (CNPq) project number 305486/2019-5; and São Paulo Research Foundation (FAPESP), grant numbers: 2021/05665-7, 2022/09164-5, and 2018/22214-6.

Declarations

Conflict of interest The authors declare no competing interests.

References

1. Altug H, Oh SH, Maier SA, Homola J. Advances and applications of nanophotonic biosensors. *Nat Nanotechnol.* 2022;17:5–16. <https://doi.org/10.1038/s41565-021-01045-5>.
2. Oliveira ONJ, Iost RM, Siqueira JRJ, Crespilho FN, Caseli L. Nanomaterials for diagnosis: challenges and applications in smart devices based on molecular recognition. *ACS Appl Mater Interfaces.* 2014;6:14745–66. <https://doi.org/10.1021/am5015056>.
3. Iost RM, da Silva WC, Madurro JM, Madurro AGB, Ferreira LF, Crespilho FN. Recent advances in nano-based electrochemical biosensors: application in diagnosis and monitoring of diseases. *Front Biosci (Elite Ed).* 2011;3:663–89. <https://doi.org/10.2741/e278>.

4. GraphenicaLab (2022). Print flexible Graphene sensors and electronic devices on any surface. <<https://graphenicalab.com/>>. Accessed 20 Aug 2022
5. Mattioli IA, Castro KR, Macedo LJA, Sedenho GC, Oliveira MN, Todeschini I, Vitale PM, Ferreira SC, Manuli ER, Pereira GM, Sabino EC, Crespilho FN. Graphene-based hybrid electrical-electrochemical point-of-care device for serologic COVID-19 diagnosis. *Biosens Bioelectron.* 2022;199:113866. <https://doi.org/10.1016/j.bios.2021.113866>.
6. Kour R, Arya S, Young S-J, Gupta V, Bandhoria P, Khosla A. Review—recent advances in carbon nanomaterials as electrochemical biosensors. *J Electrochem Soc.* 2020;167:037555. <https://doi.org/10.1149/1945-7111/ab6bc4>.
7. Ying YL, Hu ZL, Zhang S, Qing Y, Fragasso A, Maglia G, Meller A, Bayley H, Dekker C, Long YT Nanopore-based technologies beyond DNA sequencing. *Nat Nanotechnol* 2022;17: <https://doi.org/10.1038/s41565-022-01193-2>.
8. Macedo LJA, Iost RM, Hassan A, Balasubramanian K, Crespilho FN. Bioelectronics and interfaces using monolayer graphene. *ChemElectroChem.* 2019;6:31–59. <https://doi.org/10.1002/celec.201800934>.
9. Balasubramanian K, Kern K. Label-free electrical biodetection using carbon nanostructures. *Adv Mater.* 2014;26:1154–75. <https://doi.org/10.1002/adma.201304912>.
10. Kumar V, Meenakshi, Shukla SK, Thakur N Carbon-based materials approach for environmental sensing. Elsevier Inc. 2021.
11. Das CM, Kang L, Ouyang Q, Yong K-T. Advanced low-dimensional carbon materials for flexible devices. *InfoMat.* 2020;2:698–714. <https://doi.org/10.1002/inf2.12073>.
12. Candelaria SL, Shao Y, Zhou W, Li X, Xiao J, Zhang J-G, Wang Y, Liu J, Li J, Cao G. Nanostructured carbon for energy storage and conversion. *Nano Energy.* 2012;1:195–220. <https://doi.org/10.1016/j.nanoen.2011.11.006>.
13. Yu J, Song H, Li X, Tang L, Tang Z, Yang B, Lu S. Computational studies on carbon dots electrocatalysis: a review. *Adv Funct Mater.* 2021;31:2107196. <https://doi.org/10.1002/adfm.202107196>.
14. Hu C, Li M, Qiu J, Sun Y-P. Design and fabrication of carbon dots for energy conversion and storage. *Chem Soc Rev.* 2019;48:2315–37. <https://doi.org/10.1039/C8CS00750K>.
15. Wu N, Hu Q, Wei R, Mai X, Naik N, Pan D, Guo Z, Shi Z. Review on the electromagnetic interference shielding properties of carbon based materials and their novel composites: recent progress, challenges and prospects. *Carbon N Y.* 2021;176:88–105. <https://doi.org/10.1016/j.carbon.2021.01.124>.
16. Li M, Chen T, Gooding JJ, Liu J. Review of carbon and graphene quantum dots for sensing. *ACS Sensors.* 2019;4:1732–48. <https://doi.org/10.1021/acssensors.9b00514>.
17. Morales-Narváez E, Sgobbi LF, Machado SAS, Merkoçi A. Graphene-encapsulated materials: synthesis, applications and trends. *Prog Mater Sci.* 2017;86:1–24. <https://doi.org/10.1016/j.pmatsci.2017.01.001>.
18. Yang W, Ratinac KR, Ringer SR, Thordarson P, Gooding JJ, Braet F. Carbon nanomaterials in biosensors: should you use nanotubes or graphene. *Angew Chemie - Int Ed.* 2010;49:2114–38.
19. Ataíde VN, Rocha DP, de Siervo A, Paixão TRLC, Muñoz RAA, Angnes L. Additively manufactured carbon/black-integrated polylactic acid 3D printed sensor for simultaneous quantification of uric acid and zinc in sweat. *Microchim Acta.* 2021;188:388. <https://doi.org/10.1007/s00604-021-05007-5>.
20. Nascimento ED, Fonseca WT, de Oliveira TR, de Correia CRSTB, Faça VM, de Morais BP, Silvestrini VC, Pott-Junior H, Teixeira FR, Faria RC. COVID-19 diagnosis by SARS-CoV-2 spike protein detection in saliva using an ultrasensitive magneto-assay based on disposable electrochemical sensor. *Sensors Actuators B Chem.* 2022;353:131128. <https://doi.org/10.1016/j.snb.2021.131128>.
21. Botelho CN, Falcão SS, Soares R-EP, Pereira SR, de Menezes AS, Kubota LT, Damos FS, Luz RCS. Evaluation of a photo-electrochemical platform based on strontium titanate, sulfur doped carbon nitride and palladium nanoparticles for detection of SARS-CoV-2 spike glycoprotein S1. *Biosens Bioelectron X.* 2022;11:100167. <https://doi.org/10.1016/j.biosx.2022.100167>.
22. Kudr J, Zhao L, Nguyen EP, Arola H, Nevanen TK, Adam V, Zitka O, Merkoçi A. Inkjet-printed electrochemically reduced graphene oxide microelectrode as a platform for HT-2 mycotoxin immunoenzymatic biosensing. *Biosens Bioelectron.* 2020;156:112109. <https://doi.org/10.1016/j.bios.2020.112109>.
23. Yang Q, Rosati G, Abarintos V, Aroca MA, Osma JF, Merkoçi A. Wearable and fully printed microfluidic nanosensor for sweat rate, conductivity, and copper detection with healthcare applications. *Biosens Bioelectron.* 2022;202:114005. <https://doi.org/10.1016/j.bios.2022.114005>.
24. Todorova N, Makarucha AJ, Hine NDM, Mostofi AA, Yarovsky I. Dimensionality of carbon nanomaterials determines the binding and dynamics of amyloidogenic peptides: multiscale theoretical simulations. *PLOS Comput Biol.* 2013;9:e1003360.
25. Alkire RC, Bartlett PN, Lipkowsky J. *Electrochemistry of carbon electrodes.* Wiley; 2015.
26. Rao R, Pint CL, Islam AE, Weatherup RS, Hofmann S, Meshot ER, Wu F, Zhou C, Dee N, Amama PB, Carpena-Núñez J, Shi W, Plata DL, Penev ES, Jakobson BI, Balbuena PB, Bichara C, Futaba DN, Noda S, Shin H, Kim KS, Simard B, Mirri F, Pasquali M, Fornasiero F, Kauppinen EI, Arnold M, Cola BA, Nikolaev P, Arepalli S, Cheng HM, Zakharov DN, Stach EA, Zhang J, Wei F, Terrones M, Geohagan DB, Maruyama B, Maruyama S, Li Y, Adams WW, Hart AJ. Carbon nanotubes and related nanomaterials: critical advances and challenges for synthesis toward mainstream commercial applications. *ACS Nano.* 2018;12:11756–84.
27. Magna G, Mandoj F, Stefanelli M, Pomarico G, Monti D, Di Natale C, Paolesse R, Nardis S Recent Advances in Chemical Sensors Using Porphyrin-Carbon Nanostructure Hybrid Materials. *Nanomaterials* 2021; 11.
28. Ortiz-Medina J, Wang Z, Cruz-Silva R, Morelos-Gomez A, Wang F, Yao X, Terrones M, Endo M. Defect engineering and surface functionalization of nanocarbons for metal-free catalysis. *Adv Mater.* 2019;31:1805717. <https://doi.org/10.1002/adma.201805717>.
29. Holzinger M, Le GA, Cosnier S. Nanomaterials for biosensing applications: a review. 2014;2:1–10. <https://doi.org/10.3389/fchem.2014.00063>.
30. Iost RM, Crespilho FN. Layer-by-layer self-assembly and electrochemistry: applications in biosensing and bioelectronics. *Biosens Bioelectron.* 2012;31:1–10. <https://doi.org/10.1016/j.bios.2011.10.040>.
31. de Sousa Luz RA, Martins MVA, Magalhães JL, Siqueira JR, Zucolotto V, Oliveira ON, Crespilho FN, da Silva WC. Supramolecular architectures in layer-by-layer films of single-walled carbon nanotubes, chitosan and cobalt (II) phthalocyanine. *Mater Chem Phys.* 2011;130:1072–7.
32. Crespilho FN, Zucolotto V, Oliveira ON, Nart FC. Electrochemistry of layer-by-layer films: a review. *Int J Electrochem Sci.* 2006;1:194–214. <https://doi.org/10.1016/j.matchemphys.2011.08.038>.
33. Siqueira JR, Caseli L, Crespilho FN, Zucolotto V, Oliveira ON. Immobilization of biomolecules on nanostructured films for biosensing. *Biosens Bioelectron.* 2010;25:1254–63. <https://doi.org/10.1016/j.bios.2009.09.043>.

34. Iost RM, Madurro JM, Brito-Madurro AG, Nantes IL, Caseli L, Crespilho FN. Strategies of nano-manipulation for application in electrochemical biosensors. *Int J Electrochem Sci*. 2011;6:2965–97.
35. Wang H, Bai L, Chai Y, Yuan R. Synthesis of multi-fullerenes encapsulated palladium nanocage, and its application in electrochemiluminescence immunosensors for the detection of *Streptococcus suis* serotype 2. *Small*. 2014;10:1857–65. <https://doi.org/10.1002/smll.201303594>.
36. Ponomarenko LA, Schedin F, Katsnelson MI, Yang R, Hill EW, Novoselov KS, Geim AK. Chaotic Dirac billiard in graphene quantum dots. *Science*. 2008;80(320):356–8. <https://doi.org/10.1126/science.1154663>.
37. Lai S, Jin Y, Shi L, Zhou R, Zhou Y, An D. Mechanisms behind excitation- and concentration-dependent multicolor photoluminescence in graphene quantum dots. *Nanoscale*. 2020;12:591–601. <https://doi.org/10.1039/C9NR08461D>.
38. Yan Y, Chen J, Li N, Tian J, Li K, Jiang J, Liu J, Tian Q, Chen P. Systematic bandgap engineering of graphene quantum dots and applications for photocatalytic water splitting and CO₂ reduction. *ACS Nano*. 2018;12:3523–32. <https://doi.org/10.1021/acsnano.8b00498>.
39. Wang X, Feng Y, Dong P, Huang J. A mini review on carbon quantum dots: preparation, properties, and electrocatalytic application. *Front Chem*. 2019;7:671. <https://doi.org/10.3389/fchem.2019.00671>.
40. Wang J, Cao S, Ding Y, Ma F, Lu W, Sun M. Theoretical investigations of optical origins of fluorescent graphene quantum dots. *Sci Rep*. 2016;6:24850. <https://doi.org/10.1038/srep24850>.
41. Jauja-Ccana VR, Cordova-Huaman AV, Feliciano GT, La Rosa-Toro Gómez A. Experimental and molecular dynamics study of graphene oxide quantum dots interaction with solvents and its aggregation mechanism. *J Mol Liq*. 2021;335:116136. <https://doi.org/10.1016/j.molliq.2021.116136>.
42. Chahal S, Macairan J-R, Yousefi N, Tufenkji N, Naccache R. Green synthesis of carbon dots and their applications. *RSC Adv*. 2021;11:25354–63. <https://doi.org/10.1039/D1RA04718C>.
43. Shandilya R, Bhargava A, Ratre P, Kumari R, Tiwari R, Chauhan P, Mishra PK. Graphene quantum-dot-based nanophotonic approach for targeted detection of long noncoding RNAs in circulation. *ACS Omega*. 2022;7:26601–9. <https://doi.org/10.1021/acsomega.2c02802>.
44. Gao MX, Yang L, Zheng Y, Yang XX, Zou HY, Han J, Liu ZX, Li YF, Huang CZ. “Click” on alkynylated carbon quantum dots: an efficient surface functionalization for specific biosensing and bioimaging. *Chem - A Eur J*. 2017;23:2171–8. <https://doi.org/10.1002/chem.201604963>.
45. Colombo RNP. Biosensors in point-of-care: molecular analysis, strategies and perspectives to health care. In: *Advances in bioelectrochemistry*, vol. 3. Cham: Springer International Publishing; 2022. p. 169–98.
46. Alix-Panabières C, Pantel K. Liquid biopsy: from discovery to clinical application. *Cancer Discov*. 2021;11:858–73. <https://doi.org/10.1158/2159-8290.CD-20-1311>.
47. Colombo RNP, Sedenho GC, Crespilho FN. Challenges in biomaterials science for electrochemical biosensing and bioenergy. *Chem Mater*. 2022. <https://doi.org/10.1021/acscchemmater.2c02080>.
48. Lu L, Zhou L, Chen J, Yan F, Liu J, Dong X, Xi F, Chen P. Nanochannel-confined graphene quantum dots for ultrasensitive electrochemical analysis of complex samples. *ACS Nano*. 2018;12:12673–81. <https://doi.org/10.1021/acsnano.8b07564>.
49. Gao N, Yang W, Nie H, Gong Y, Jing J, Gao L, Zhang X. Turn-on theranostic fluorescent nanoprobe by electrostatic self-assembly of carbon dots with doxorubicin for targeted cancer cell imaging, in vivo hyaluronidase analysis, and targeted drug delivery. *Biosens Bioelectron*. 2017;96:300–7. <https://doi.org/10.1016/j.bios.2017.05.019>.
50. Mansuriya BD, Altintas Z. Enzyme-free electrochemical nano-immunosensor based on graphene quantum dots and gold nanoparticles for cardiac biomarker determination. *Nanomaterials*. 2021;11:578. <https://doi.org/10.3390/nano11030578>.
51. Fan D, Bao C, Khan MS, Wang C, Zhang Y, Liu Q, Zhang X, Wei Q. A novel label-free photoelectrochemical sensor based on N, S-GQDs and CdS co-sensitized hierarchical Zn₂SnO₄ cube for detection of cardiac troponin I. *Biosens Bioelectron*. 2018;106:14–20. <https://doi.org/10.1016/j.bios.2018.01.050>.
52. Hu T, Zhang L, Wen W, Zhang X, Wang S. Enzyme catalytic amplification of miRNA-155 detection with graphene quantum dot-based electrochemical biosensor. *Biosens Bioelectron*. 2016;77:451–6. <https://doi.org/10.1016/j.bios.2015.09.068>.
53. Ajgaonkar R, Lee B, Valimukhametova A, Nguyen S, Gonzalez-Rodriguez R, Coffey J, Akkaraju GR, Naumov AV. Detection of pancreatic cancer miRNA with biocompatible nitrogen-doped graphene quantum dots. *Materials (Basel)*. 2022;15:5760. <https://doi.org/10.3390/ma15165760>.
54. Chung S, Revia RA, Zhang M. Graphene quantum dots and their applications in bioimaging, biosensing, and therapy. *Adv Mater*. 2021;33:1904362. <https://doi.org/10.1002/adma.201904362>.
55. Ratre P, Jain B, Kumari R, Thareja S, Tiwari R, Srivastava RK, Goryacheva IY, Mishra PK. Bioanalytical applications of graphene quantum dots for circulating cell-free nucleic acids: a review. *ACS Omega*. 2022. <https://doi.org/10.1021/acsomega.2c05414>.
56. Long D, Li M, Wang H, Wang H, Chai Y, Yuan R. A photoelectrochemical biosensor based on fullerene with methylene blue as a sensitizer for ultrasensitive DNA detection. *Biosens Bioelectron*. 2019;142:111579. <https://doi.org/10.1016/j.bios.2019.111579>.
57. Afreen S, Muthoosamy K, Manickam S, Hashim U. Functionalized fullerene (C₆₀) as a potential nanomediator in the fabrication of highly sensitive biosensors. *Biosens Bioelectron*. 2015;63:354–64. <https://doi.org/10.1016/j.bios.2014.07.044>.
58. Pilehvar S, De Wael K. Recent advances in electrochemical biosensors based on fullerene-C₆₀ nano-structured platforms. In: *Nanocarbons for electroanalysis*. John Wiley & Sons, Ltd, Chichester, UK., 2017; pp 173–196.
59. Turcheniuk K, Mochalin VN. Biomedical applications of nanodiamond (review). *Nanotechnology*. 2017;28:252001. <https://doi.org/10.1088/1361-6528/aa6ae4>.
60. Arora N, Sharma NN. Arc discharge synthesis of carbon nanotubes: comprehensive review. *Diam Relat Mater*. 2014;50:135–50. <https://doi.org/10.1016/j.diamond.2014.10.001>.
61. Duclaux L. Review of the doping of carbon nanotubes (multiwalled and single-walled). *Carbon N Y*. 2002;40:1751–64. [https://doi.org/10.1016/S0008-6223\(02\)00043-X](https://doi.org/10.1016/S0008-6223(02)00043-X).
62. Hong S, Lee D-M, Park M, Wee J-H, Jeong HS, Ku B-C, Yang C-M, Lee DS, Terrones M, Kim YA, Hwang JY. Controlled synthesis of N-type single-walled carbon nanotubes with 100% of quaternary nitrogen. *Carbon N Y*. 2020;167:881–7. <https://doi.org/10.1016/j.carbon.2020.06.027>.
63. Charlier J-C. Defects in carbon nanotubes. *Acc Chem Res*. 2002;35:1063–9. <https://doi.org/10.1021/ar010166k>.
64. Bachilo SM, Strano MS, Kittrell C, Hauge RH, Smalley RE, Weisman RB. Structure-assigned optical spectra of single-walled carbon nanotubes. *Science*. 2002;80(298):2361–6. <https://doi.org/10.1126/science.1078727>.
65. Gong K, Chakrabarti S, Dai L. Electrochemistry at carbon nanotube electrodes: is the nanotube tip more active than the sidewall? *Angew Chemie Int Ed*. 2008;47:5446–50. <https://doi.org/10.1002/anie.200801744>.

66. Kiciński W, Dyjak S. Transition metal impurities in carbon-based materials: pitfalls, artifacts and deleterious effects. *Carbon N Y*. 2020;168:748–845. <https://doi.org/10.1016/j.carbon.2020.06.004>.
67. Li T, Liang Y, Li J, Yu Y, Xiao M-M, Ni W, Zhang Z, Zhang G-J. Carbon nanotube field-effect transistor biosensor for ultrasensitive and label-free detection of breast cancer exosomal miRNA21. *Anal Chem*. 2021;93:15501–7. <https://doi.org/10.1021/acs.analchem.1c03573>.
68. Zamzami MA, Rabbani G, Ahmad A, Basalah AA, Al-Sabban WH, Nate Ahn S, Choudhry H. Carbon nanotube field-effect transistor (CNT-FET)-based biosensor for rapid detection of SARS-CoV-2 (COVID-19) surface spike protein S1. *Bioelectrochemistry*. 2022;143:107982. <https://doi.org/10.1016/j.bioelechem.2021.107982>.
69. Chen H, Xiao M, He J, Zhang Y, Liang Y, Liu H, Zhang Z. Aptamer-functionalized carbon nanotube field-effect transistor biosensors for Alzheimer's disease serum biomarker detection. *ACS Sensors*. 2022;7:2075–83. <https://doi.org/10.1021/acssensors.2c00967>.
70. Chen M, Wu D, Tu S, Yang C, Chen D, Xu Y. A novel biosensor for the ultrasensitive detection of the lncRNA biomarker MALAT1 in non-small cell lung cancer. *Sci Rep*. 2021;11:3666. <https://doi.org/10.1038/s41598-021-83244-7>.
71. Langenbacher R, Budhathoki-Uprety J, Jena PV, Roxbury D, Streit J, Zheng M, Heller DA. Single-chirality near-infrared carbon nanotube sub-cellular imaging and FRET probes. *Nano Lett*. 2021;21:6441–8. <https://doi.org/10.1021/acs.nanolett.1c01093>.
72. Loeian MS, Mehdi Aghaei S, Farhadi F, Rai V, Yang HW, Johnson MD, Aqil F, Mandadi M, Rai SN, Panchapakesan B. Liquid biopsy using the nanotube-CTC-chip: capture of invasive CTCs with high purity using preferential adherence in breast cancer patients. *Lab Chip*. 2019;19:1899–915. <https://doi.org/10.1039/C9LC00274J>.
73. Martins MVA, Pereira AR, Luz RAS, Iost RM, Crespilho FN. Evidence of short-range electron transfer of a redox enzyme on graphene oxide electrodes. *Phys Chem Chem Phys*. 2014;16:17426–36. <https://doi.org/10.1039/c4cp00452c>.
74. Carrière M, Henrique M Buzzetti P, Gorgy K, Giroud F, Li H, Borsali R, Cosnier S Nanostructured electrodes based on multiwalled carbon nanotube/glyconanoparticles for the specific immobilization of bilirubin oxidase: application to the electrocatalytic O₂ reduction. *Bioelectrochemistry*. 2022; 108328. <https://doi.org/10.1016/j.bioelechem.2022.108328>.
75. Olivares F, Peón F, Henríquez R, del Río RS. Strategies for area-selective deposition of metal nanoparticles on carbon nanotubes and their applications: a review. *J Mater Sci*. 2022;57:2362–87. <https://doi.org/10.1007/s10853-021-06710-7>.
76. Dai B, Zhou R, Ping J, Ying Y, Xie L. Recent advances in carbon nanotube-based biosensors for biomolecular detection. *TrAC Trends Anal Chem*. 2022;154:116658. <https://doi.org/10.1016/j.trac.2022.116658>.
77. Antonucci A, Reggente M, Roullier C, Gillen AJ, Schuergers N, Zubkovs V, Lambert BP, Mouhib M, Carata E, Dini L, Boghossian AA. Carbon nanotube uptake in cyanobacteria for near-infrared imaging and enhanced bioelectricity generation in living photovoltaics. *Nat Nanotechnol*. 2022;17:1111–9. <https://doi.org/10.1038/s41565-022-01198-x>.
78. Geim AK, Novoselov KS. The rise of graphene. *Nat Mater*. 2007;6:183–91. <https://doi.org/10.1038/nmat1849>.
79. Novoselov KS, Geim AK, Morozov S V., Jiang D, Zhang Y, Dubonos S V., Grigorieva I V., Firsov AA (2004) Electric field in atomically thin carbon films. *Science*. 2004; (80). <https://doi.org/10.1126/science.1102896>.
80. Compton RG. Saying what we mean. *Electrochem Commun*. 2016;64:A1. <https://doi.org/10.1016/j.elecom.2016.02.010>.
81. Yi M, Shen Z. A review on mechanical exfoliation for the scalable production of graphene. *J Mater Chem A*. 2015;3:11700–15. <https://doi.org/10.1039/c5ta00252d>.
82. Song J, Kam FY, Png RQ, Seah WL, Zhuo JM, Lim GK, Ho PKH, Chua LL. A general method for transferring graphene onto soft surfaces. *Nat Nanotechnol*. 2013. <https://doi.org/10.1038/nnano.2013.63>.
83. Mattevi C, Kim H, Chhowalla M. A review of chemical vapour deposition of graphene on copper. *J Mater Chem*. 2011;21:3324–34. <https://doi.org/10.1039/c0jm02126a>.
84. Lai SCS, Patel AN, McKelvey K, Unwin PR. Definitive evidence for fast electron transfer at pristine basal plane graphite from high-resolution electrochemical imaging. *Angew Chemie - Int Ed*. 2012. <https://doi.org/10.1002/anie.201200564>.
85. Yadav A, Wehrhold M, Neubert TJ, Iost RM, Balasubramanian K. Fast Electron transfer kinetics at an isolated graphene edge nanoelectrode with and without nanoparticles: implications for sensing electroactive species. *ACS Appl Nano Mater*. 2020. <https://doi.org/10.1021/acsnm.0c02171>.
86. Yadav A, Iost RM, Neubert TJ, Baylan S, Schmid T, Balasubramanian K. Selective electrochemical functionalization of the graphene edge. *Chem Sci*. 2019. <https://doi.org/10.1039/c8sc04083d>.
87. Neubert TJ, Krieg J, Yadav A, Balasubramanian K. pH sensitivity of edge-gated graphene field-effect devices with covalent edge functionalization. *ACS Appl Electron Mater*. 2022. <https://doi.org/10.1021/acsaem.2c00880>.
88. Toth PS, Valota AT, Velický M, Kinloch IA, Novoselov KS, Hill EW, Dryfe RAW. Electrochemistry in a drop: a study of the electrochemical behaviour of mechanically exfoliated graphene on photoresist coated silicon substrate. *Chem Sci*. 2014;5:582–9. <https://doi.org/10.1039/c3sc52026a>.
89. Velický M, Bradley DF, Cooper AJ, Hill EW, Kinloch IA, Mishchenko A, Novoselov KS, Patten HV, Toth PS, Valota AT, Worrall SD, Dryfe RAW. Electron transfer kinetics on mono- and multilayer graphene. *ACS Nano*. 2014;8:10089–100. <https://doi.org/10.1021/nn504298r>.
90. Li X, Magnuson CW, Venugopal A, Tromp RM, Hannon JB, Vogel EM, Colombo L, Ruoff RS. Large-area graphene single crystals grown by low-pressure chemical vapor deposition of methane on copper. *J Am Chem Soc*. 2011;133:2816–9. <https://doi.org/10.1021/ja109793s>.
91. Zhou H, Yu WJ, Liu L, Cheng R, Chen Y, Huang X, Liu Y, Wang Y, Huang Y, Duan X. Chemical vapour deposition growth of large single crystals of monolayer and bilayer graphene. *Nat Commun*. 2013;4:4–11. <https://doi.org/10.1038/ncomms3096>.
92. Wu T, Zhang X, Yuan Q, Xue J, Lu G, Liu Z, Wang H, Wang H, Ding F, Yu Q, Xie X, Jiang M. Fast growth of inch-sized single-crystalline graphene from a controlled single nucleus on Cu-Ni alloys. *Nat Mater*. 2016;15:43–7. <https://doi.org/10.1038/nmat4477>.
93. Zuccaro L, Krieg J, Desideri A, Kern K, Balasubramanian K. Tuning the isoelectric point of graphene by electrochemical functionalization. *Sci Rep*. 2015. <https://doi.org/10.1038/srep11794>.
94. Wang QH, Jin Z, Kim KK, Hilmer AJ, Paulus GLC, Shih CJ, Ham MH, Sanchez-Yamagishi JD, Watanabe K, Taniguchi T, Kong J, Jarillo-Herrero P, Strano MS. Understanding and controlling the substrate effect on graphene electron-transfer chemistry via reactivity imprint lithography. *Nat Chem*. 2012;4:724–32. <https://doi.org/10.1038/nchem.1421>.
95. Macedo LJA, Lima FCDA, Amorim RG, Freitas RO, Yadav A, Iost RM, Balasubramanian K, Crespilho FN. Interplay of non-uniform charge distribution on the electrochemical modification of graphene. *Nanoscale*. 2018;10:15048–57. <https://doi.org/10.1039/c8nr03893g>.

96. Bélanger D, Pinson J. Electrografting: a powerful method for surface modification. *Chem Soc Rev*. 2011. <https://doi.org/10.1039/c0cs00149j>.
97. Zuccaro L, Kern K, Balasubramanian K. Identifying chemical functionalization on individual carbon nanotubes and graphene by local vibrational fingerprinting. *ACS Nano*. 2015. <https://doi.org/10.1021/acs.nano.5b00479>.
98. Šljukić B, Banks CE, Compton RG. Iron oxide particles are the active sites for hydrogen peroxide sensing at multiwalled carbon nanotube modified electrodes. *Nano Lett*. 2006;6:1556–8. <https://doi.org/10.1021/nl060366v>.
99. Banks CE, Compton RG. Exploring the electrocatalytic sites of carbon nanotubes for NADH detection: an edge plane pyrolytic graphite electrode study. *Analyst*. 2005. <https://doi.org/10.1039/b508702c>.
100. Ambrosi A, Chee SY, Khezri B, Webster RD, Sofer Z, Pumera M. Metallic impurities in graphenes prepared from graphite can dramatically influence their properties. *Angew Chemie - Int Ed*. 2012;51:500–3. <https://doi.org/10.1002/anie.201106917>.
101. Iost RM, Crespilho FN, Zuccaro L, Yu HK, Wodtke AM, Kern K, Balasubramanian K. Enhancing the electrochemical and electronic performance of CVD-grown graphene by minimizing trace metal impurities. *ChemElectroChem*. 2014;1:2070–4. <https://doi.org/10.1002/celec.201402325>.
102. Cui C, Lim ATO, Huang J. A cautionary note on graphene anti-corrosion coatings. *Nat Nanotechnol*. 2017;12:834–5. <https://doi.org/10.1038/nnano.2017.187>.
103. Gonçalves WD, Iost RM, Crespilho FN. Diffusion mechanisms in nanoelectrodes: evaluating the edge effect. *Electrochim Acta*. 2014;123:66–71. <https://doi.org/10.1016/j.electacta.2013.12.160>.
104. Kim SN, Kuang Z, Slocik JM, Jones SE, Cui Y, Farmer BL, McAlpine MC, Naik RR. Preferential binding of peptides to graphene edges and planes. *J Am Chem Soc*. 2011;133:14480–3. <https://doi.org/10.1021/ja2042832>.
105. Zuccaro L, Tesaro C, Kurkina T, Fiorani P, Yu HK, Knudsen BR, Kern K, Desideri A, Balasubramanian K. Real-time label-free direct electronic monitoring of topoisomerase enzyme binding kinetics on graphene. *ACS Nano*. 2015. <https://doi.org/10.1021/acs.nano.5b05709>.
106. Pampaloni NP, Lottner M, Giugliano M, Matruglio A, D'Amico F, Prato M, Garrido JA, Ballerini L, Scaini D. Single-layer graphene modulates neuronal communication and augments membrane ion currents. *Nat Nanotechnol*. 2018;13:755–64. <https://doi.org/10.1038/s41565-018-0163-6>.
107. Iost RM, Sales FCPF, Martins MVA, Almeida MC, Crespilho FN. Glucose biochip based on flexible carbon fiber electrodes: in vivo diabetes evaluation in rats. *ChemElectroChem*. 2015. <https://doi.org/10.1002/celec.201402339>.
108. Lee H, Choi TK, Lee YB, Cho HR, Ghaffari R, Wang L, Choi HJ, Chung TD, Lu N, Hyeon T, Choi SH, Kim DH. A graphene-based electrochemical device with thermoresponsive microneedles for diabetes monitoring and therapy. *Nat Nanotechnol*. 2016. <https://doi.org/10.1038/nnano.2016.38>.
109. Lee H, Hong YJ, Baik S, Hyeon T, Kim DH. Enzyme-based glucose sensor: from invasive to wearable device. *Adv Healthc Mater*. 2018;7:1–14. <https://doi.org/10.1002/adhm.201701150>.
110. Choi C, Lee Y, Cho KW, Koo JH, Kim DH. Wearable and implantable soft bioelectronics using two-dimensional materials. *Acc Chem Res*. 2019;52:73–81. <https://doi.org/10.1021/acs.accounts.8b00491>.
111. Traversi F, Raillon C, Benameur SM, Liu K, Khlybov S, Tosun M, Krasnozhan D, Kis A, Radenovic A. Detecting the translocation of DNA through a nanopore using graphene nanoribbons. *Nat Nanotechnol*. 2013;8:939–45. <https://doi.org/10.1038/nnano.2013.240>.
112. Mannoor MS, Tao H, Clayton JD, Sengupta A, Kaplan DL, Naik RR, Verma N, Omenetto FG, McAlpine MC. Graphene-based wireless bacteria detection on tooth enamel. *Nat Commun*. 2012; 3: <https://doi.org/10.1038/ncomms1767>.
113. Mattioli IA, Hassan A, Sanches NM, Vieira NCS, Crespilho FN. Highly sensitive interfaces of graphene electrical-electrochemical vertical devices for on drop atto-molar DNA detection. *Biosens Bioelectron*. 2021;175:112851. <https://doi.org/10.1016/j.bios.2020.112851>.
114. Seo G, Lee G, Kim MJ, Baek S-H, Choi M, Ku KB, Lee C-S, Jun S, Park D, Kim HG, Kim S-J, Lee J-O, Kim BT, Park EC, Il KS. Rapid detection of COVID-19 causative virus (SARS-CoV-2) in human nasopharyngeal swab specimens using field-effect transistor-based biosensor. *ACS Nano*. 2020. <https://doi.org/10.1021/acs.nano.0c02823>.
115. Mattioli IA, Crespilho FN. Problems of interpreting diagnostic tests for SARS-CoV-2: analytical chemistry concerns. *An Acad Bras Cienc*. 2020;92:1–3. <https://doi.org/10.1590/0001-376520202021208>.
116. Mattioli IA, Hassan A, Oliveira ON Jr, Crespilho FN, Oliveira ON, Crespilho FN. On the challenges for the diagnosis of SARS-CoV-2 based on a review of current methodologies. *ACS Sensors*. 2020;5:3655–77. <https://doi.org/10.1021/acssensors.0c01382>.
117. Hassan A, Macedo LJA, Mattioli IA, Rubira RJG, Constantino CJL, Amorim RG, Lima FCDA, Crespilho FN. A three component-based van der Waals surface vertically designed for biomolecular recognition enhancement. *Electrochim Acta*. 2021;376:138025. <https://doi.org/10.1016/j.electacta.2021.138025>.
118. Sanches NM, Hassan A, Mattioli IA, Macedo LJA, Sedenho GC, Crespilho FN. Tuning vertical electron transfer on graphene bilayer electrochemical devices. *Adv Mater Interfaces*. 2021;8:2100550. <https://doi.org/10.1002/admi.202100550>.
119. Swinya DL, Martín-Yerga D, Walker M, Unwin PR. Surface Nanostructure effects on dopamine adsorption and electrochemistry on glassy carbon electrodes. *J Phys Chem C*. 2022;126:13399–408. <https://doi.org/10.1021/acs.jpcc.2c02801>.
120. Gonçalves VR, Colombo RNP, Minadeo MAOS, Matsubara EY, Rosolen JM, Córdoba de Torresi SI. Three-dimensional graphene/carbon nanotubes hybrid composites for exploring interaction between glucose oxidase and carbon based electrodes. *J Electroanal Chem*. 2016;775:235–42. <https://doi.org/10.1016/j.jelechem.2016.06.002>.
121. Cheng Z, Liu Y, Meng C, Dai Y, Luo L, Liu X. Constructing a weaving structure for aramid fiber by carbon nanotube-based network to simultaneously improve composites interfacial properties and compressive properties. *Compos Sci Technol*. 2019;182:107721. <https://doi.org/10.1016/j.compscitech.2019.107721>.
122. Baccarin M, Santos FA, Vicentini FC, Zucolotto V, Janegitz BC, Fatibello-Filho O. Electrochemical sensor based on reduced graphene oxide/carbon black/chitosan composite for the simultaneous determination of dopamine and paracetamol concentrations in urine samples. *J Electroanal Chem*. 2017;799:436–43. <https://doi.org/10.1016/j.jelechem.2017.06.052>.
123. Nagar B, Balsells M, de la Escosura-Muñiz A, Gomez-Romero P, Merkoçi A. Fully printed one-step biosensing device using graphene/AuNPs composite. *Biosens Bioelectron*. 2019;129:238–44. <https://doi.org/10.1016/j.bios.2018.09.073>.
124. Stankovich S, Dikin DA, Dommett GHB, Kohlhaas KM, Zimney EJ, Stach EA, Piner RD, Nguyen ST, Ruoff RS. Graphene-based composite materials. *Nature*. 2006;442:282–6. <https://doi.org/10.1038/nature04969>.
125. Kinloch IA, Suhr J, Lou J, Young RJ, Ajayan PM. Composites with carbon nanotubes and graphene: an outlook. *Science*. 2018;80(362):547–53. <https://doi.org/10.1126/science.aat7439>.
126. de Souza JCP, Iost RM, Crespilho FN. Nitrated carbon nanoblenders for high-performance glucose dehydrogenase bioanodes.

- Biosens Bioelectron. 2016;77:860–5. <https://doi.org/10.1016/j.bios.2015.08.069>.
127. Han Q, Wang A, Song W, Zhang M, Wang S, Ren P, Hao L, Yin J, Bai S. Fabrication of conductive, adhesive, and stretchable agarose-based hydrogels for a wearable biosensor. *ACS Appl Bio Mater*. 2021;4:6148–56. <https://doi.org/10.1021/acsabm.1c00501>.
128. Macedo LJA, Hassan A, Sedenho GC, Crespilho FN. Assessing electron transfer reactions and catalysis in multicopper oxidases with operando X-ray absorption spectroscopy. *Nat Commun*. 2020;11:316. <https://doi.org/10.1038/s41467-019-14210-1>.
129. Cheng R, Colombo RNP, Zhang L, Nguyen DHT, Tilley R, Cordoba de Torresi SI, Dai L, Gooding JJ, Gonçalves VR. Porous graphene oxide films prepared via the breath-figure method: a simple strategy for switching access of redox species to an electrode surface. *ACS Appl Mater Interfaces*. 2020;12:55181–8. <https://doi.org/10.1021/acsami.0c16811>.
130. Sedenho GC, Neckel IT, Colombo RNP, Pacheco JC, Bertaglia T, Crespilho FN Investigation of water splitting reaction by a multicopper oxidase through X-ray absorption nanospectroelectrochemistry. *Adv Energy Mater* n/a.2022; 2202485. <https://doi.org/10.1002/aenm.202202485>.
131. Singh M, Nolan H, Tabrizian M, Cosnier S, Düsberg GS, Holzinger M. Functionalization of contacted carbon nanotube forests by dip coating for high-performance biocathodes. *ChemElectroChem*. 2020;7:4685–9. <https://doi.org/10.1002/celec.202001334>.
132. Buzzetti PHM, Blanchard P-Y, Giroto EM, Nishina Y, Cosnier S, Le Goff A, Holzinger M. Insights into carbon nanotube-assisted electro-oxidation of polycyclic aromatic hydrocarbons for mediated bioelectrocatalysis. *Chem Commun*. 2021;57:8957–60. <https://doi.org/10.1039/D1CC02958D>.
133. Berezovska A, Nedellec Y, Giroud F, Gross AJ, Cosnier S. Free-standing biopellet electrodes based on carbon nanotubes and protein compression for direct and mediated bioelectrocatalysis. *Electrochem Commun*. 2021;122:106895. <https://doi.org/10.1016/j.elecom.2020.106895>.
134. Mordor Intelligence. Carbon nanotubes market - growth, trends, COVID-19 impact, and forecasts (2022 - 2027).
135. Precedence Research. Carbon nanotubes market - growth, trends, COVID-19 impact, and forecasts (2022 - 2027).
136. Meunier V, Ania C, Bianco A, Chen Y, Choi GB, Kim YA, Koratkar N, Liu C, Tascon JMD, Terrones M. Carbon science perspective in 2022: current research and future challenges. *Carbon N Y*. 2022;195:272–91. <https://doi.org/10.1016/j.carbon.2022.04.015>.
137. Hansen SF, Lennquist A. Carbon nanotubes added to the SIN List as a nanomaterial of Very High Concern. *Nat Nanotechnol*. 2020;15:3–4. <https://doi.org/10.1038/s41565-019-0613-9>.
138. Heller DA, Jena PV, Pasquali M, Kostarelos K, Delogu LG, Meidl RE, Rotkin SV, Scheinberg DA, Schwartz RE, Terrones M, Wang Y, Bianco A, Boghossian AA, Cambré S, Cognet L, Corrie SR, Demokritou P, Giordani S, Hertel T, Ignatova T, Islam MF, Iverson NM, Jagota A, Janas D, Kono J, Kruss S, Landry MP, Li Y, Martel R, Maruyama S, Naumov AV, Prato M, Quinn SJ, Roxbury D, Strano MS, Tour JM, Weisman RB, Wenseleers W, Yudasaka M. Banning carbon nanotubes would be scientifically unjustified and damaging to innovation. *Nat Nanotechnol*. 2020;15:164–6. <https://doi.org/10.1038/s41565-020-0656-y>.

Publisher's note Springer Nature remains neutral with regard to jurisdictional claims in published maps and institutional affiliations.

Springer Nature or its licensor (e.g. a society or other partner) holds exclusive rights to this article under a publishing agreement with the author(s) or other rightsholder(s); author self-archiving of the accepted manuscript version of this article is solely governed by the terms of such publishing agreement and applicable law.